Plant Pathology (2013) Doi: 10.1111/ppa.12106

Effect of wheat spike infection timing on fusarium head blight development and mycotoxin accumulation

D. Siou[a]*, S. Gélisse[a], V. Laval[a], C. Repinçay[b], R. Canalès[c], F. Suffert[a] and C. Lannou[a]

[a]*INRA, UMR1290 BIOGER, F-78850 Thiverval-Grignon;* [b]*INRA, UR 251 PESSAC, RD 10, F-78026 Versailles Cedex; and* [c]*Bayer CropScience France, 16 rue Jean marie Leclair, 69266 Lyon, France*

Fusarium head blight in wheat spikes is associated with production of mycotoxins by the fungi. Although flowering is recognized as the most favourable host stage for infection, a better understanding of infection timing on disease development and toxin accumulation is needed. This study monitored the development of eight characterized isolates of *F. graminearum*, *F. culmorum* and *F. poae* in a greenhouse experiment. The fungi were inoculated on winter wheat spikes before or at anther extrusion, or at 8, 18 and 28 days later. Disease levels were estimated by the AUDPC and thousand-kernel weight (TKW). The fungal biomass (estimated by qPCR) and toxin concentration (deoxynivalenol and nivalenol, estimated by UPLC-UV-MS/MS) were measured in each inoculated spike, providing a robust estimation of these variables and allowing correlations based on single-individual measurements to be established. The toxin content correlated well with fungal biomass in kernels, independently of inoculation date. The AUDPC was correlated with fungal DNA, but not for early and late infection dates. The highest disease and toxin levels were for inoculations around anthesis, but early or late infections led to detectable levels of fungus and toxin for the most aggressive isolates. Fungal development appeared higher in kernels than in the chaff for inoculations at anthesis, but the opposite was found for later inoculations. These results show that anthesis is the most susceptible stage for FHB, but also clearly shows that early and late infections can produce significant disease development and toxin accumulation with symptoms difficult to estimate visually.

Keywords: flowering date, *Fusarium culmorum*, *Fusarium graminearum*, *Fusarium poae*, toxin productivity

Introduction

Fusarium head blight (FHB) is one of the most destructive diseases of wheat. It is distributed worldwide and caused by several species of the genus *Fusarium* and *Microdochium*. Among the 19 species identified as potentially responsible for FHB, *F. graminearum*, *F. culmorum*, *F. avenaceum*, *F. poae*, *M. nivale* and *M. majus* are the most frequent in Europe (Ioos *et al.*, 2005; Xu & Nicholson, 2009). FHB induces quantitative yield losses and can result in the contamination of the kernels with mycotoxins such as deoxynivalenol (DON) or nivalenol (NIV) (McMullen *et al.*, 1997). Anthesis is the most susceptible stage for *Fusarium* infection, especially when anthers are mature and begin to senesce (Parry *et al.*, 1995). At anthesis, the opening of the florets allows the fungal hyphae to establish infection more easily (Brown *et al.*, 2010). Moreover, anthers contain high levels of nutrients that are known to stimulate the growth of *Fusarium* hyphae (Strange *et al.*, 1974).

The fungus can infect the plant through other ways such as the adaxial surface of the glumes, the lemma or the palea or even through a wound in the chaff (Bai & Shaner, 1994; Goswami & Kistler, 2004; Brown *et al.*, 2010). In the field, spore production and release from infected debris can occur anytime before and after flowering, as long as the climatic conditions are favourable. This potentially extends the plant receptivity period and might explain the recurrent observations of high DON content in spikes with relatively few symptoms (Del Ponte *et al.*, 2003, 2007; Hallen-Adams *et al.*, 2011). Several studies point out the fact that wheat spike contamination at stages later than flowering can occur and result in healthy-appearing kernels that contain toxins, especially when moisture conditions are high (Hart *et al.*, 1984; Cowger *et al.*, 2009). For instance, late infections resulting in high DON levels in the harvested kernels have been observed in field conditions in France, in 2007, and were attributed to humid conditions at the end of the wheat cycle. That year, FHB severity and toxin contents were largely underestimated by the forecast models, which tend to ignore the risk of late infections.

The impact of late contaminations on disease development and toxin production has been explored by Cowger & Arrellano (2010), who inoculated eight winter wheat cultivars with four *F. graminearum* isolates, from 0 to 20 days after mid-anthesis. The period of maximum receptivity was around 10 days after mid-anthesis, while the occurrence of rain after anthesis extended the normal

*E-mail: dorothee.siou@hotmail.fr

window of susceptibility and was conducive to the low-symptom, high-DON scenario. These results are consistent with other studies. Hart *et al.* (1984) infected wheat spikes with one isolate of *F. graminearum*, both in controlled conditions and in the field, with inoculation time ranging from watery to mid-dough stage. DON was produced in wheat spikes under favourable moisture conditions, even at late stages of kernel development, whereas yield reductions were greatest when infections occurred before kernel filling. In a controlled-environment study, Del Ponte *et al.* (2007) inoculated a *F. graminearum* isolate on spikes of a wheat cultivar at six stages from mid-anthesis to hard dough. The percentage of damaged kernels was >94% for inoculations performed between mid-anthesis and late milk stages but fell to 23% for inoculation at hard dough. The highest DON concentrations were found in samples inoculated at the watery-ripe and early milk stages but DON was still detected at later stages, without significant reductions of the kernel weight. However, other authors reached different conclusions. Using several species of *Fusarium*, Lacey *et al.* (1999) inoculated a winter wheat cultivar at different times from spike emergence to harvest. Little or no disease and DON production were observed for inoculations performed between spike emergence and the start of anthesis. Anthesis was the only infection time for which high DON concentrations were observed and both disease severity and DON content sharply decreased for inoculations performed after mid-anthesis.

The papers reviewed above suggest that late infections may to some extent allow fungal development and toxin production. To further explore this question, this study attempted to more specifically relate the fungus development with the toxin content in the kernels by using accurate quantification techniques (qPCR for fungal DNA estimation and liquid chromatography and mass spectrometry for toxin quantification) and by working at the spike level for all measurements. This allowed better estimation of the disease severity at late development stages of the spike, when plant senescence makes symptom quantification by visual assessment difficult. Moreover, assessing both the fungal DNA and the toxin content in the same spikes made it possible to precisely correlate the observable disease severity, the level of kernel colonization by the fungus, and the toxin production. As it is still unclear whether the different species composing the FHB complex present the same risk in terms of late infection and toxin production, the experiments involved three species of the FHB complex in Europe, *F. graminearum*, *F. culmorum* and *F. poae*.

Materials and methods

Plant material

A greenhouse experiment was carried out in 2010 and replicated in 2011. Seeds of winter wheat cv. Royssac, considered to be highly susceptible to FHB, were sown in Jiffy peat pots and kept for 2 weeks under greenhouse conditions for seedling emergence. Seedlings were vernalized in a growth chamber for 8 weeks at 8°C with a 10 h-day photoperiod. They were then individually transplanted into pots filled with 1 L commercial compost (Klasmann Peat Substrat 4; Klasmann France SARL), with 2 g of slow-release fertilizer (Osmocote Exact 16-11-11 N-P-K 3MgO Te). Pots were placed in a greenhouse compartment at 15–20°C and under a 15 h-day photoperiod. During plant growth, natural daylight was supplemented with 400 W sodium lights between 06:00 and 21:00 h. Plants were fertilized with Hydrokani C2 (Hydro Agri Spécialités) at a 1:100 dilution rate. In each pot, only the main tiller was maintained. For each plant, the flowering date of the spike was recorded. The plants were sprayed with metrafenone (Flexity at 1 mL L^{-1}; Bayer CropScience) and lambda-cyhalothrine (Karaté Zéon at 0·2 mL L^{-1}; Syngenta Agro S.A.S.) as a preventive measure to control powdery mildew (*Blumeria graminis*) and insects, respectively. These pesticides have been tested in other experiments and have no detectable effect on FHB.

Fungal material

The list of fungal isolates used in the experiments is summarized in Table 1. The *F. graminearum* and *F. culmorum* isolates were provided by F. Forget (INRA Bordeaux, France) and the *F. poae* isolates were provided by R. Canalès (Bayer CropScience, France). They all originate from field samplings in France. For spore production, the isolates were grown in Petri dishes on

Table 1 Isolates of *Fusarium* spp. used in the experiments

Code	Species	Chemotype[a]	Aggressiveness[b]	Year of experiment	
				2010	2011
fg159	*F. graminearum*	DON	+	+	+
fg178	*F. graminearum*	DON	+++	+	+
fg165	*F. graminearum*	DON	+++	+	–
fc124	*F. culmorum*	DON	+++	+	+
fc129	*F. culmorum*	NIV	++	+	+
fp2	*F. poae*	NIV	–	+	–
fp3	*F. poae*	NIV	–	+	–
fp6	*F. poae*	NIV	–	–	+

[a]Main toxin produced. The chemotype has been established in previous experiments for *F. graminearum* and *F. culmorum* and in the present experiment for *F. poae*.

[b]Average aggressiveness as measured on wheat spikes in the greenhouse in other experiments.

potato dextrose agar (PDA, 39 g L^{-1}) at 19°C and kept in the light for 3 days. Four mycelial plugs were then transferred in 250 mL of CMC medium. After at least 3 days with continual shaking, the medium was filtered through cheesecloth to collect the spores. For each isolate, a spore suspension in sterile distilled water was adjusted to a concentration of 2×10^4 conidia mL^{-1} using a Malassez cell. Suspensions were then stored at 4°C until they were used for inoculation, which took place within the same day. After inoculation, a few microlitres of each spore suspension was deposited on PDA to check for spore viability.

Experimental design and inoculation procedure

The experiment was conducted in autumn 2010 and repeated in 2011 with the same cultivar and using the same protocols for inoculation, disease assessment and toxin analysis. For each isolate and date of inoculation, eight to nine spikes were inoculated on main tillers, each in a different pot. The pots were randomized in the greenhouse. Four dates of inoculation were tested: F0, anther extrusion (appearance of the first extruded anthers); F8, eight days post-anther extrusion (dpae); F18 (18 dpae), corresponding to the milky kernel development stage; and F28 (28 dpae), corresponding to the dough development stage (Zadoks *et al.*, 1974). In the 2011 experiment only, additional inoculations were performed before flowering and anther extrusion (FX). For the FX treatment, the appearance of the first anthers sometimes occurred during the incubation time and the corresponding spikes were then reassigned to the F0 class. The spikes were inoculated using an atomizer (Ecospray; Prolabo). Inoculation consisted of spraying each side of a spike with 1 mL of inoculum suspension. After spraying, the spikes were enclosed for 3 days in a transparent polyethylene bag sealed to maintain 100% relative humidity and promote infection. The average relative humidity in the greenhouse during the whole experiment was 80%.

Disease assessment

The spikes were observed from 5 days after inoculation (appearance of the first symptoms) until 25 days after inoculation. The number of spikelets with FHB symptoms was visually assessed three times a week. As the aspect of FHB symptoms may vary, each spikelet with symptoms showing a premature bleaching or brown necrosis was putatively considered as diseased and this status was confirmed or not at the following assessment date. The percentage of diseased spikelets on each spike was calculated. The dynamics of appearance of spikelets with symptoms on each spike was characterized by the area under the disease progression curve (AUDPC), calculated from the observation of first symptoms to 15 days after inoculation.

At maturity, the spikes were cut and hand-threshed to separate each kernel from the chaff. Kernels were then weighed to estimate the thousand-kernel weight (TKW). The status (symptomless or diseased) of each kernel was assessed to evaluate the percentage of damaged kernels per spike. A kernel was considered damaged when showing tombstone-like symptoms, white mycelium or discoloration. After visual observation, the kernels of each spike were ground with a mixer mill (MM 400, Retsch) and stored for DNA and toxin quantification.

In order to explain the relatively high amount of toxins in the kernels of some spikes inoculated at late growth stages in 2010, the hypothesis that the mycelium present in the chaff could be a source of toxins for the kernels was tested. The chaff of five spikes inoculated at F8 and F18 with each isolate of *F. graminearum* and *F. culmorum* were ground for DNA analysis. The low quantities of plant material obtained after the chaff grinding did not allow quantification of the toxins in these samples.

Detection and quantification of fungal DNA

The fungal DNA in the kernels was estimated by quantitative PCR (qPCR), which is considered an accurate technique for assessing the fungal development in the kernels (Nicolaisen *et al.*, 2008; Nielsen *et al.*, 2011).

DNA extraction

The total DNA was extracted from around 50 mg of ground material using the DNeasy Plant Mini Kit (QIAGEN) according to the manufacturer's instructions, with a slightly modified version. In short, flour was vortexed with 400 μL AP1 buffer, 4 μL RNase and 4 μL proteinase K solution (20 mg mL^{-1}) before incubation at 65°C for 1 h. Samples were homogenized for 10 to 15 min during the incubation. After that, 260 μL AP2 buffer were added and samples were incubated on ice for 10 min. The tubes were centrifuged at 18 000 ***g*** for 5 min. The supernatant was then transferred to purple columns and centrifuged at 18 000 ***g*** for 2 min. In new tubes, 750 μL AP3/ethanol buffer were added to the supernatant. After homogenization by tube inversion, 650 μL of this mix were transferred to white columns and centrifuged at 6000 *g* for 1 min. This step was repeated with the leftover of extracts. The DNA pellet, trapped in the white column was washed with 500 μL AW/ethanol buffer and a centrifugation at 6000 ***g*** for 1 min and this wash was repeated with a centrifugation at 18 000 ***g*** for 2 min. Then, DNA was eluted by adding 50 μL AE buffer and, after an incubation of 5 min at room temperature, centrifuged at 6000 ***g*** for 1 min. This step was repeated twice. The DNA was quantified with a NanoDrop ND-1000 spectrophotometer (NanoDrop Technology) and diluted to a final concentration of 20 ng μL^{-1}.

qPCR quantification

The amount of both fungal and wheat DNA was estimated by quantitative PCR (qPCR). Species-specific primer pairs and species-specific TaqMan probes were used to enhance the specificity of the test (Siou, 2013; V. Laval, personal communication, INRA, Thiverval-Grignon, France). The primers and probes were purchased from Eurogentec. Primers were designed using the OLIGO v. 6 primer analysis Software. Probes were designed using PRIMER EXPRESS, v. 2.0 (Applied Biosystems). All the probes used were TaqMan-labelled with FAM/TAMRA quencher. Real-time PCR was carried out in a total of 25 μL consisting of 6·25 μL qPCR MasterMix with ROX and uracil-N-glycosylase (UNG) at a final concentration of 1× (Eurogentec), 300 nM each primer, 100 nM of species-specific probe and 5 μL template DNA at 20 ng μL^{-1}. The samples were standardized based on the plant DNA quantified with plant EF-1α real-time PCR primers, as described in Nicolaisen *et al.* (2008). For wheat DNA quantification, the MESA GREEN qPCR MasterMix Plus for SYBR Assay (Eurogentec) was used at a final concentration of 1×, with the same concentration of each primer and 5 μL template DNA diluted 1:10. The PCR reactions were performed in duplicate on all samples, and in triplicate on samples used for the standard curve, on ABI PRISM 7900 Sequence Detection System (Applied Biosystems) in Applied Biosystem 96-well plates. The amplification conditions included: an initial step of 2 min at 50°C; 95°C for 10 min; and 40 cycles of 15 s at 95°C and 60 s at 62°C (60°C for *F. poae*). DNA quantifications were done using standard curves of DNA from *F. graminearum*,

F. culmorum, *F. poae* or wheat extracted from pure cultures and non-contaminated wheat kernels. Each standard curve was generated by tenfold dilution series ranging from 1·0 to 1×10^{-3} ng μL^{-1} for fungal DNA and 5·0 to 5×10^{-3} ng μL^{-1} for wheat DNA. Results were analysed using AB SDS v. 2.2.2 software (Applied Biosystem). PCR efficiency was on average 98·0% and ranged between 94·0 and 100%. As described by Nicolaisen *et al.* (2008), the amount of fungal DNA was calculated from cycle threshold (C_t) values using the standard curve, and these values were normalized with the estimated amount of plant DNA based on the plant EF-1α assay.

Detection and quantification of mycotoxins

Toxin standards were purchased from Sigma. The water used for all extraction and ultraperformance liquid chromatography (UPLC) was purified in a milli-Q integral water purification system (EMD Millipore). All other chemicals and solvents were HPLC grade, except methanol used for UPLC analysis which was LCMS grade (Carlo Erba). Only DON and NIV were quantified.

Toxin extraction

A homogenized flour sample of around 1 g was used for toxin extraction for five of the eight replicates of each treatment. Flour samples were frozen and vacuum dried using a freeze-drier to evaluate the moisture of each sample. This flour was shaken for 1·5 h at room temperature in 6·0 mL acetonitrile–water (84:16, v/v). The suspension was centrifuged at 7000 ***g*** for 10 min, and 4·0 mL of the supernatant were collected. These extracts were evaporated to dryness using a SpeedVac Concentrator (Eppendorf) at 45°C for 2 h and then 60°C. The dried samples were dissolved in 200 μL methanol and sonicated for 10 min in an ultrasound bath. Water (800 μL) was added before a second sonication for 10 min in an ultrasound bath. To avoid flour residues, the samples were centrifuged at 7000 ***g*** for 10 min and only the clear supernatant was taken for UPLC-UV-MS/MS analysis. For the most concentrated samples, the supernatant was diluted 5, 10 or 20 times in a methanol–water solution (20:80).

UPLC-UV-MS/MS conditions

The UPLC-UV-MS/MS analysis of the toxin extract was performed with an Acquity ultraperformance liquid chromatograph (UPLC) coupled with a TQD tandem mass spectrometer (MS) (Waters Corp.). Instrument monitoring and data processing were performed using MASSLYNX v. 4.1 (Waters). Chromatographic separation was carried out with an EC 100/2 NUCLEODUR C18 gravity column (Macherey-Nagel GmbH & Co.; 100 mm × 2 mm i.d., 1·8 μm particle size) at a flow rate of 0·33 mL min^{-1}. The column was maintained at 30°C and the sample manager was kept at 10°C. A volume of 10 μL of toxin extract was injected. The sample injection needle and loop were flushed with 200 μL methanol followed by 600 μL methanol–water (5:95, v/v). Mobile phases used were: A, water and B, methanol, both supplemented with 5 mM ammonium acetate. The gradient conditions were summarized in Table S1.

The mass spectrometer was operated in electrospray ionization (ESI negative ion mode) under multiple-reaction monitoring mode (MRM). The parameters influencing the MS signal were optimized individually for each compound by continuously infusing a standard solution at 10 μg mL^{-1} in acetonitrile into the mass spectrometer. The resulting optimized values were as follows: capillary voltage, 3 kV; source and desolvation temperatures, 120°C and 450°C, respectively. Nitrogen, obtained from pressurized air in a nitrogen generator (Zefiro 35 LC-MS, F-DBS) was used at 50 and 600 L h^{-1} for cone and desolvation gas, respectively; argon (99·9999% purity, Air Liquide) was used as collision gas with a pressure of $2{\cdot}5 \times 10^{-3}$ mbar in the collision cell (T-Wave). Dwell times varying between 0·125 and 0·3 s were selected in order to obtain at least 15 points per peak. The MRM transitions for each compound and the corresponding optimized parameters (cone voltage and collision energy) are listed in Table S2.

Identification of the target analytes was accomplished by comparing the retention time and the UPLC-UV-MS/MS signals of the compounds in the samples with those of standards analysed under identical conditions. For each analyte, two MS/MS signals were monitored corresponding to the two most abundant transitions: the most abundant one was to quantify the analytes and the less abundant one to confirm their identity. For the quantification, the external standard method was used, with standard solutions containing a mixture of DON and NIV in acetonitrile. Concentrations ranged from 0·002 to 5·0 mg L^{-1}.

Results were then converted to mg g^{-1} of dry biomass with the following equation: toxin concentration = ([X × V × DF × 6/4] / DW), where X is the concentration given by the software in mg L^{-1}, V is the final toxin extract volume (0·001 L), DF is a dilution factor, and DW is the dry weight of flour. The value 6/4 corresponds to the 4 mL collected from the 6 mL acetonitrile–water added to the flour for the toxin extraction. The limit of detection and quantification for both toxins were all $<2 \times 10^{-6}$ mg g^{-1}.

Data analysis

The toxin productivity was calculated as the quantity of toxin produced per unit of fungal DNA (Simpson *et al.*, 2004). Variance analyses were used to determine the effects of the inoculation date, the experiment, the species and the isolate (nested within the species) on AUDPC, TKW, the fungal DNA and the toxin content of the kernels. Tukey's HSD test was used for the multiple mean comparisons. Residuals distribution was checked for linearity and variance homogeneity. Regression analyses were used to explore the relationship between the visual disease assessment, the fungal biomass and the toxin content. In the following, it is considered that the fungal DNA is an estimation of the fungal biomass in the samples.

Results

Correlations between variables

Over all samples, the toxin concentration and the fungal DNA were highly correlated ($r = 0{\cdot}85$, $P < 0{\cdot}001$; Fig. 1). A covariance analysis (Table 2), with the fungal DNA as a co-variable, showed a strong effect of the fungal DNA, the isolate and the inoculation date on the toxin concentration. However, there was no significant interaction between the inoculation date and the fungal DNA, indicating that the toxin concentration–fungal biomass relationship was independent of the inoculation date. The slope of the linear regression of toxin concentration on fungal DNA is a measure of the toxin productivity. The analysis then indicates that the inoculation date, and thus the stage at which the infection took place, did not influence the toxin productivity. The

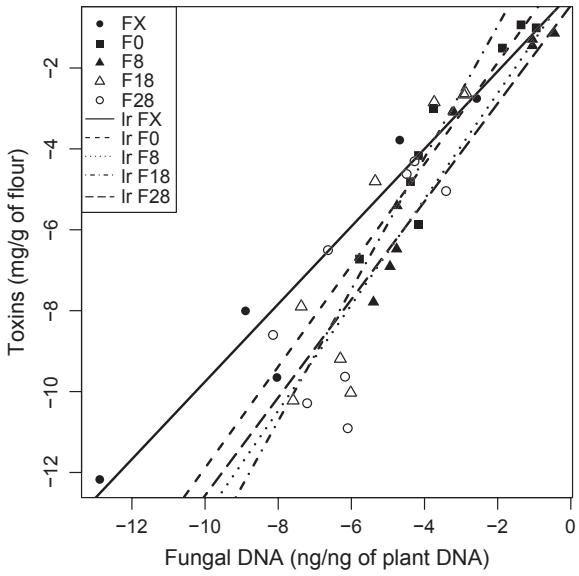

Figure 1 Correlation between toxin concentration and fungal DNA in wheat spikes inoculated with several *Fusarium* strains at five different dates (FX, F0, F8, F18 and F28, respectively 3 days before anther extrusion and 0, 8, 18 and 28 days post-anther extrusion). The fungal DNA and the toxin content were determined in each individual spike. The data are log-transformed. For clarity, only the average values for an isolate (over replicates and experiments) are represented on the figures. The lines show linear regressions (lr) for each inoculation date, based on all replicates of both experiments (see Table 2 for a detailed ANCOVA analysis including the different factors of variation).

experiment as a main factor had no effect on the toxin concentration but the interaction between experiment and fungal DNA influenced the toxin concentration. Nevertheless, this interaction, as well as the others that were detected in this analysis, only accounted for a small part of the global variance in toxin concentration and did not change the general conclusion of a clear link between toxin concentration and fungal biomass (Fig. 1), independent of the time of inoculation.

The AUDPC was found to be highly correlated to the fungal DNA for inoculations performed at F0 and F8 ($r = 0{\cdot}70$, $P < 0{\cdot}001$ and $r = 0{\cdot}84$, $P < 0{\cdot}001$, respectively) but this correlation became weaker for F18 ($r = 0{\cdot}62$, $P < 0{\cdot}001$) and was not significant at FX and F28 ($r = 0{\cdot}16$, $P = 0{\cdot}11$ and $r = 0{\cdot}13$, $P = 0{\cdot}21$, respectively; Fig. 2). The covariance analysis (Table 2) revealed a significant interaction between the slope of the relationship and the inoculation date, confirming that the link between visual symptoms, denoted by AUDPC, and the fungal biomass in the kernels varies with the stage at which the spikes are inoculated. The experiment had a significant and strong effect on the AUDPC, indicating that uncontrolled changes in the environment between the 2010 and 2011 experiments influenced the disease development. The TKW gave roughly the same information as the AUDPC, except that the experiment accounted for a lower part of the variance than it did for AUDPC (data not shown).

Table 2 Analysis of the relationships between fungal DNA and toxin content, and fungal DNA and AUDPC. The ANCOVA includes the fungal DNA as a co-variable and the inoculation date (Date), the experiment (Exp) and the isolate (Iso) as explanatory factors

Source of variation	df	MS	*F*-value	*P*-value
Toxin content				
Date (A)[a]	4	148·42	216·60	<0·001
Fungal DNA (B)	1	262·37	382·89	<0·001
Exp (C)[b]	1	0·22	0·32	0·575
Iso (D)[c]	7	189·32	276·29	<0·001
A × B	4	1·07	1·56	0·186
A × C	3	4·99	7·28	<0·001
B × C	1	10·25	14·95	<0·001
A × D	25	3·19	4·66	<0·001
B × D	7	3·87	5·65	<0·001
C × D	3	8·70	12·69	<0·001
Residuals	179	0·69		
AUDPC				
Date (A)[a]	4	1·186	50·39	<0·001
Fungal DNA (B)	1	1·064	45·21	<0·001
Exp (C)[b]	1	5·147	218·69	<0·001
Iso (D)[c]	7	2·908	123·56	<0·001
A × B	4	0·236	10·01	<0·001
A × C	3	0·654	27·77	<0·001
B × C	1	0·006	0·24	0·624
A × D	25	0·261	11·07	<0·001
B × D	7	0·101	4·31	<0·001
C × D	3	0·100	4·25	0·006
Residuals	379	0·024		

[a]Inoculation date (FX, F0, F8, F18 or F28).
[b]Experiment (2010 or 2011).
[c]Isolate inoculated (see Table 1).

Species effect

The species effect, with the isolate as a nested effect, was tested in an ANOVA analysis on the different measured variables (Table 3). Multiple mean comparisons showed that *F. poae* was less aggressive than the two other species, with lower disease severity values ($P < 0{\cdot}001$ for AUDPC, TKW and fungal DNA) and produced less toxins ($P < 0{\cdot}001$). Interactions were detected between the species and other factors (inoculation date and experiment), but they resulted only from slight changes in the mean values, and did not change the main conclusion that *F. poae* was less aggressive than the two other species. No significant difference was observed between *F. graminearum* and *F. culmorum* at the species level. The following focuses on the date and isolate effects.

Effect of inoculation date on disease development and toxin production

AUDPC, TKW, fungal DNA and toxin concentration were influenced by the inoculation date and by the isolate (Table 3). Except for the toxin concentration, they were also influenced by the experiment. The interaction between the isolate and the inoculation date and between the isolate and the experiment were significant.

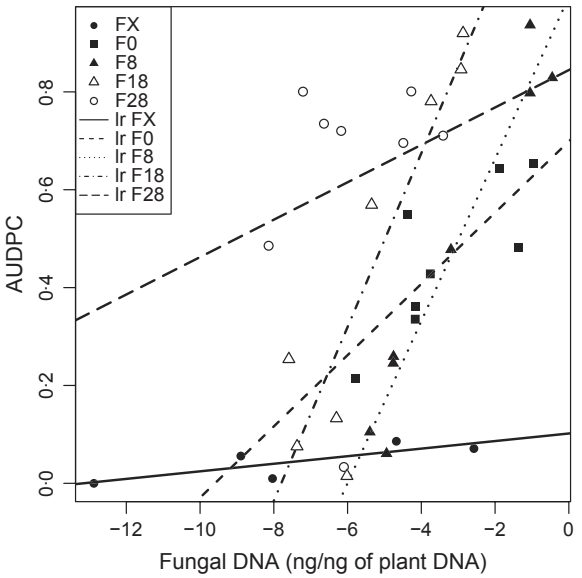

Figure 2 Correlation between AUDPC and fungal DNA in wheat spikes inoculated with several *Fusarium* strains at five different dates (FX, F0, F8, F18 and F28, respectively 3 days before anther extrusion and 0, 8, 18 and 28 days post-anther extrusion). The fungal DNA was determined in each individual spike. The data are log-transformed. For clarity, only the average values for an isolate (over replicates and experiments) are represented on the figures. The lines show linear regressions (lr) for each inoculation date, based on all replicates of both experiments (see Table 2 for a detailed ANCOVA analysis including the different factors of variation).

Nevertheless, the inoculation date, the species, and the isolate (within the species) together accounted for 82, 66 and 84% of the variance of TKW, fungal DNA and toxin concentration, respectively.

Because of the interactions between the isolate and other factors, the effect of the inoculation date was tested separately for each isolate. For the most aggressive isolates (fg178, fg165, fc124 and fc129, rated ++ or +++ in Table 1), significantly ($P < 0{\cdot}05$) higher fungal DNA and toxin concentrations were found for inoculation dates F0 and F8 than for the other dates, and the TKW significantly ($P < 0{\cdot}001$) increased from F0 to F28 (Fig. 3). This pattern was less clear for AUDPC, with high values still measured for the last inoculation dates (F18 and F28). The non-aggressive isolates (fg159, fp2, fp3 and fp6) produced less disease (as denoted by both AUDPC and fungal DNA) and less toxin. However, for those isolates, significantly higher levels were detected for the fungal DNA and the toxin content, either for F0 or for F8, depending on the isolate. Regarding TKW, the pattern was less clear than for the aggressive isolates, but fp2 still showed an increasing tendency (except for F28). High AUDPC values were measured for the last inoculation date (F28), except for fp6, which can be explained by a visual confusion between head blight symptoms and natural spike maturation.

Table 3 Variance analyses showing the effects of the inoculation date (Date), the experiment (Exp), the species and the isolate (Iso) on AUDPC, TKW, fungal DNA, toxin concentration and toxin productivity

Source of variance	df	MS	*F*-value	*P*-value
AUDPC				
Date (A)[a]	4	2·279	73·71	<0·001
Species (B)	2	3·632	117·48	<0·001
Exp (C)[b]	1	3·743	121·05	<0·001
Iso in species (D)[c]	5	2·378	76·90	<0·001
A × B	8	0·423	13·68	<0·001
A × C	3	0·499	16·14	<0·001
B × C	1	0·299	9·67	0·002
A × D	17	0·158	5·13	<0·001
C × D	2	0·328	10·62	<0·001
Residuals	404	0·031		
TKW				
Date (A)	4	5092	64·35	<0·001
Species (B)	2	4389	55·46	<0·001
Exp (C)	1	636	8·04	0·005
Iso in species (D)	5	1628	20·57	<0·001
A × B	8	553	6·99	<0·001
A × C	3	405	5·12	0·002
B × C	1	20	0·25	0·616
A × D	17	424	5·36	<0·001
C × D	2	401	5·06	0·007
Residuals	401	79		
Fungal DNA				
Date (A)	4	1·4387	29·06	<0·001
Species (B)	2	1·3017	26·29	<0·001
Exp (C)	1	0·4727	9·55	0·002
Iso in species (D)	5	1·4204	28·69	<0·001
A × B	8	0·2739	5·53	<0·001
A × C	3	0·0579	1·17	0·321
B × C	1	0·0021	0·04	0·836
A × D	17	0·3430	6·93	<0·001
C × D	2	1·0265	20·74	<0·001
Residuals	400	0·0495		
Toxin concentration				
Date (A)	4	0·3366	49·61	<0·001
Species (B)	2	0·2841	41·87	<0·001
Exp (C)	1	0·0030	0·44	0·509
Iso in species (D)	5	0·2773	40·86	<0·001
A × B	8	0·0539	7·94	<0·001
A × C	3	0·0084	1·24	0·298
B × C	1	0·0005	0·08	0·783
A × D	17	0·0625	9·21	<0·001
C × D	2	0·0389	5·74	0·004
Residuals	210	0·0068		
Toxin productivity				
Date (A)	4	380·9	1·69	0·153
Species (B)	2	692·4	3·08	0·048
Exp (C)	1	445·9	1·98	0·161
Iso in species (D)	5	278·8	1·24	0·292
A × B	8	286·3	1·27	0·260
A × C	3	538·5	2·39	0·070
B × C	1	336·3	1·50	0·223
A × D	17	255·8	1·14	0·321
C × D	2	940·7	4·18	0·017
Residuals	203	225		

[a]Inoculation date (FX, F0, F8, F18 or F28).
[b]Experiment (2010 or 2011).
[c]Isolate inoculated (see Table 1).

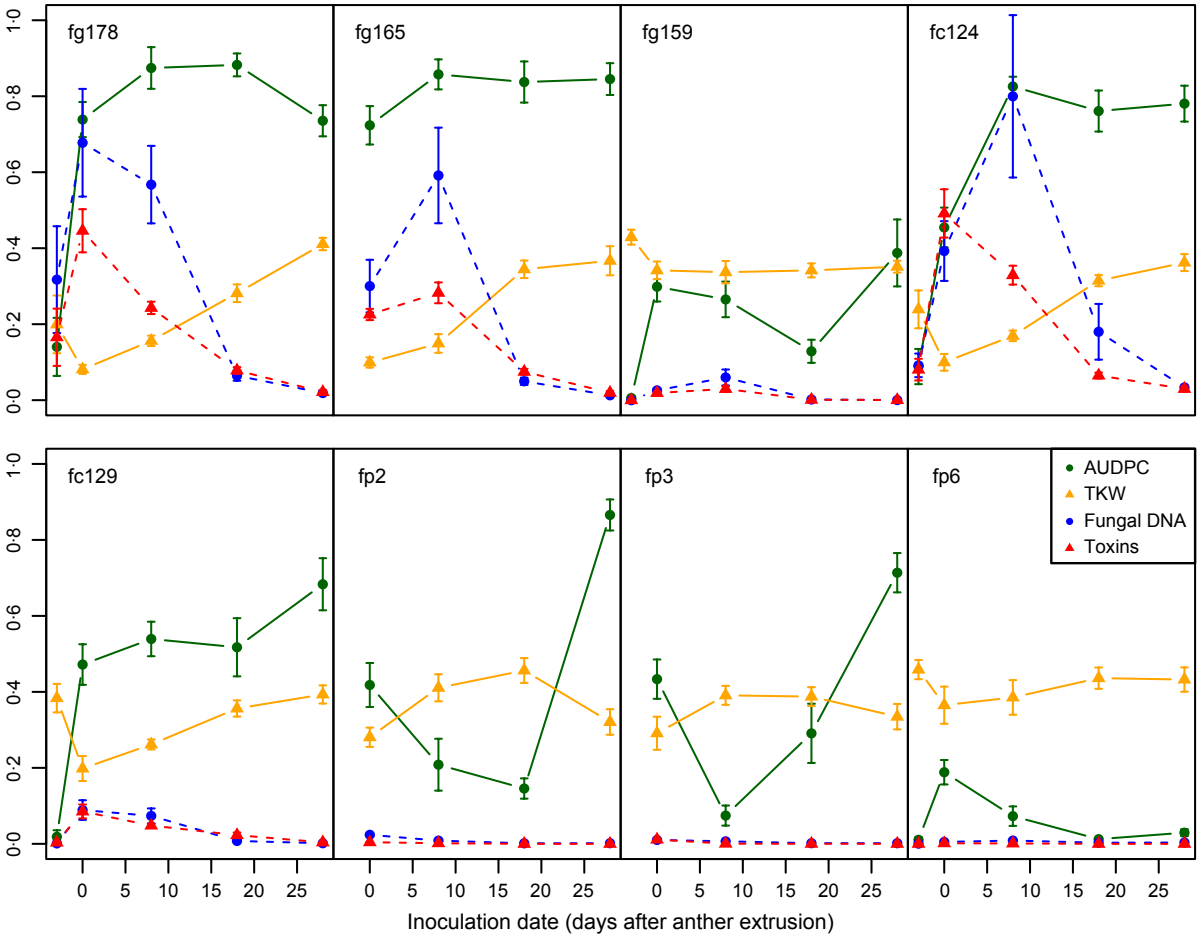

Figure 3 Variations of AUDPC (green circles), TKW (in g/100, yellow triangles), fungal DNA (blue circles, dashed lines) and toxin concentration (red triangles, dashed lines), according to the inoculation date (FX, F0, F8, F18 and F28, respectively 3 days before anther extrusion and 0, 8, 18 and 28 days post-anther extrusion). The wheat spikes were inoculated with different isolates of three *Fusarium* species (see Table 1). Data from the 2010 and 2011 experiments are averaged. A complete ANOVA analysis on the same data is presented in Table 3.

Even if the fungal biomass and the toxin concentrations in the kernels were low for the F18 and F28 treatments, they were detected at a quantifiable level for all aggressive isolates in each inoculated spike, and their average value was significantly greater than zero (Student's *t*-test, $P < 0{\cdot}05$).

Inoculations performed before flowering (FX, in the 2011 experiment) resulted in a lower disease severity (AUDPC and fungal DNA) and lower toxin concentrations in the kernels than those made at F0 and F8 (Fig. 3). In this treatment, the disease progression was slower than for F0 and F8: at first a few localized symptoms were observed, followed by a slow colonization of the spikes (Fig. 4). This denotes a lower infection efficiency, followed by a limited spike colonization. As for the F18 and F28 treatments, a quantifiable level of fungal DNA was detected here for fg178 and fc124 in each inoculated spike.

Overall, no difference was found in toxin productivity between the different inoculation dates (Table 3), confirming the conclusion of the analysis of the fungal DNA–toxin concentration relationship (Table 2). However, in some replicates the toxin production was unexpectedly high for F18, compared to F8. Even though the average differences in productivity were finally found not significant, the hypothesis that a high fungal development in the glumes and rachis could have been a source of toxins for the kernels was tested. The amount of fungal DNA in the chaff of the F8 and F18 replicates was then measured. The fungal DNA measured in the chaff was not significantly different for F8 and F18 but the variance analysis revealed a significant effect of the tissue (kernel or chaff) in which the fungal DNA was quantified (Table 4). Interestingly, there was a significant interaction between tissue and inoculation date, indicating that the fungal DNA was higher in the kernels than in the chaff for F8 but was higher in the chaff than in the kernels for F18.

Discussion

A unique feature of this study is that the disease assessment (AUDPC, TKW and fungal biomass) and the toxin

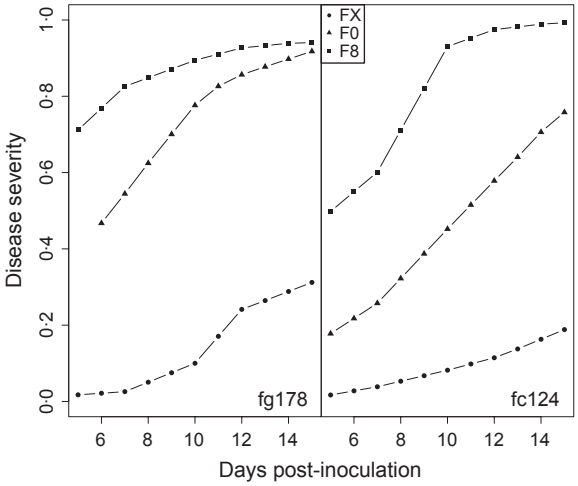

Figure 4 Kinetics of FHB development (disease severity, or fraction of the spike covered with symptoms, as a function of the number of days after inoculation) for the FX treatment (inoculation 3 days before anther extrusion), compared to the F0 and F8 treatments (inoculation at anther extrusion and 8 days post-anther extrusion, respectively). The figure details the kinetics of disease development for two of the isolates (fg178 and fc124) for which the AUDPC is shown in Figure 3. The symbols are indicated on the figure. Each point represents the average of eight replicates.

Table 4 Variance analyses showing the effect of the inoculation date (Date), the isolate (Iso) and the plant tissue analysed (Tissue) on the fungal DNA

Source of variance	df	MS	*F*-value	*P*-value
Fungal DNA				
Date (A)[a]	1	1·402	50·33	<0·001
Iso (B)[b]	4	0·2767	9·93	<0·001
Tissue (C)[c]	1	0·136	4·88	0·029
A × B	4	0·1275	4·58	0·002
A × C	1	0·6263	22·48	<0·001
B × C	4	0·0267	0·96	0·432
Residuals	120	0·0279		

[a]Inoculation date (F8 and F18).
[b]Isolate inoculated (only the *F. graminearum* and the *F. culmorum* isolates).
[c]Plant tissue analysed (kernels or chaff).

quantification were performed spike by spike, which provided a robust estimation of these parameters. The use of a separate qPCR analysis for each spike allowed a precise quantification of the within-host fungal development. Because the development of FHB at the scale of an individual spike is highly variable, mixing different spikes for toxin analysis or for DNA quantification leads to a lower precision in the treatment comparisons than working entirely at the spike level. This gain in precision made it possible to measure significant fungal development and toxin contamination for late inoculation dates and to clearly distinguish aggressive from non-aggressive isolates.

Another feature of this study is the comparison of isolates of three different species, including *F. poae*, a fungus of increasingly recognized importance, for which very few experimental studies have so far been published (Stenglein, 2009). *Fusarium poae* is considered to be a relatively weak pathogen compared to *F. graminearum* and *F. culmorum* (Brennan *et al.*, 2003; Stenglein, 2009). The data in the present study are in accordance with this view: significantly lower disease severity, fungal DNA and toxin concentrations were obtained with *F. poae* isolates, compared to *F. culmorum* and *F. graminearum*. In contrast, no significant difference in pathogenicity was found between *F. culmorum* and *F. graminearum* in the present experiments, even though isolate fg159 appeared to have particularly low aggression. However, the low number of isolates per species that were tested does not allow a general conclusion to be drawn at the species level.

A good correlation was found between the fungal DNA and the toxin concentration, and the stage at which the spikes were inoculated did not alter this correlation. Figure 1, along with the ANOVA analysis (Table 3), indicates that the toxin productivity did not significantly change with the timing of inoculation relative to spike maturation, even though the fungal development was considerably lower for late inoculations. However, the presence of a significant isolate × fungal DNA interaction suggests that not all isolates expressed the same toxin productivity. In addition, the toxin productivity was slightly influenced by environmental effects (experiment × fungal DNA interaction).

For both *F. graminearum* and *F. culmorum*, it was found that the fungal DNA was less abundant in the chaff than in the kernels for inoculations at anthesis (F8), whereas the opposite was true for later inoculations (F18). Such a difference has already been observed. In spontaneous field epidemics, Xu *et al.* (2008) found that the fungal DNA was significantly more abundant in the chaff than in the kernels at harvest. As mentioned by Leonard & Bushnell (2003), the water content decreases and the pericarp cell walls thicken during kernel maturation, which renders infection more difficult for the fungus. This may explain why the fungus tends to colonize other tissues more at late development stages. Another possible explanation is that the fungus has easier access to host nutriments in the chaff than in the maturated kernels at this stage of plant development. However, in the present experiments, there is no indication that the fungal development in the chaff influenced the toxin level in the kernels.

The AUDPC is a common measure used to estimate the disease level in a crop. Here, the correlation between the AUDPC (based on visual symptoms) and the fungal biomass was high for inoculations performed around anthesis (F0 and F8) but rather low or even not significant for earlier or later inoculation dates. The visual assessment of disease on the spike thus appeared to be a poor estimator of the actual infection level for those early or late infections. Such a discrepancy between visual assessments and actual infection level may explain

why disease severity and toxin concentrations are sometimes poorly correlated (Alvarez *et al.*, 2010). Regarding the late infections, a likely explanation is that FHB symptoms can be visually confused with natural spike maturation, leading to an overestimation of FHB severity. Another possible cause is that the fungus seems to develop better in the glumes than in the kernels for late infection dates (Xu *et al.*, 2008), which might increase the level of externally visible symptoms. The findings here that the amount of fungal DNA was higher in the chaff than in the kernels for inoculations at F18 supports this idea.

When the inoculations were performed before anthesis (FX treatment), a few localized symptoms were observed at the first assessment date, followed by a slow colonization of the spikes (see Fig. 4). This probably denotes a lower infection efficiency than for the infections performed around anthesis but it shows that infection, followed by some level of spike colonization, is nevertheless possible when contamination occurs before flowering. Gourdain & Rosengarten (2011) have found in a field experiment that inoculations performed before heading can lead to an observable disease development. The presence of already established infections before flowering may pose a risk of fast disease development if the weather conditions later become favourable to the mycelium development.

The infection timing strongly conditioned the attack intensity on kernels, with increasing values of TKW from F0 to F28, especially for inoculations performed with aggressive isolates. The data are in good accordance with the widely accepted fact that F0 and F8 correspond to the most favourable period for FHB infection. Several authors suggest or have shown that this results from a better access to the flower tissues for the fungus, especially through extruded anthers (Hart *et al.*, 1984; Bai & Shaner, 1994). Nevertheless, the fungal DNA and toxin concentration obtained for FX and for late inoculations (F18 and F28) were clearly above the detection level in each spike inoculated with an aggressive strain, and were on average significantly greater than zero. This suggests that early infections as well as late infections can lead to a certain level of fungal colonization and toxin production in the spike.

Hallen-Adams *et al.* (2011) showed that the toxin production may extend over a long period after infection and can still occur in mature kernels. Hart *et al.* (1984) and Cowger *et al.* (2009) also demonstrated that DON can be produced in wheat when there is adequate moisture for fungal growth, regardless of the kernels' stage. In the present experiments, the spikes were not exposed to a high relative humidity after the incubation period and this explains the low toxin content observed for F18 and F28. The presence of the fungus at a detectable level in these treatments nevertheless suggests that, given suitable moisture conditions, higher toxin levels could be obtained, leading to a low-symptom, high-DON scenario. Another possible consequence of late infections is the production of infected kernels that nevertheless keep a good germination capacity. At the next season, this can lead to the development of fusarium foot rot. More generally, the presence of infected seeds can participate in increasing the level of inoculum in the soil for the following years.

This work confirms the well established result that anthesis is the critical window for FHB infection but it also shows that a later infection with an aggressive *Fusarium* isolate may lead to significant development of the fungus, along with accumulation of toxins in the kernels, and with symptoms that are very difficult to evaluate visually. Although early or late contaminations led to relatively low disease levels that would probably not impact the yield in the field conditions, such late infections may lead to higher toxin concentrations when the climatic conditions are favourable (Cowger *et al.*, 2009). Moreover, late kernel contamination might have consequences for seed production because they lead to viable but infected kernels. Fungicide applications and FHB risk assessments, which are today focused on a narrow window around flowering, might be improved by taking into account later development stages when environmental conditions are favourable. To quote Del Ponte *et al.* (2003), "We need to consider integrated strategies that will protect wheat spikes from infection for several weeks rather than several days after flowering".

Acknowledgements

The authors are grateful to Bayer CropScience for their financial support and to the Ile de France region for their contribution to the UPLC-UV-MS/MS purchase. They thank F. Forget for providing fungal isolates, M. Bourdat-Deschamps for her help in the toxin analysis and B. Beauzoone and M. Willigsecker for their technical help. Financial support was provided by the ANR DON&co project.

References

Alvarez CL, Somma S, Moretti A, Fernandez Pinto V, 2010. Aggressiveness of *Fusarium graminearum sensu stricto* isolates in wheat kernels in Argentina. *Journal of Phytopathology* **158**, 173–81.

Bai G, Shaner G, 1994. Scab of wheat: prospects for control. *Plant Disease* **78**, 760–6.

Brennan JM, Fagan B, Van Maanen A, Cooke BM, Doohan FM, 2003. Studies on *in vitro* growth and pathogenicity of European *Fusarium* fungi. *European Journal of Plant Pathology* **109**, 577–87.

Brown NA, Urban M, Van De Meene AML, Hammond-Kosack KE, 2010. The infection biology of *Fusarium graminearum*: defining the pathways of spikelet to spikelet colonisation in wheat spikes. *Fungal Biology* **114**, 555–71.

Cowger C, Arrellano C, 2010. Plump kernels with high deoxynivalenol linked to late *Gibberella zeae* infection and marginal disease conditions in winter wheat. *Phytopathology* **100**, 719–28.

Cowger C, Patton-Özkurt J, Brown-Guedira G, Perugini L, 2009. Post-anthesis moisture increased *Fusarium* head blight and deoxynivalenol levels in North Carolina winter wheat. *Phytopathology* **99**, 320–7.

Del Ponte EM, Fernandes JMC, Bergstrom GC, 2003. *Fusarium* head blight and deoxynivalenol accumulation in wheat inoculated at developmental stages from flowering through grain maturation. In:

Canty SM, Lewis J, Siler L, Ward RW, eds. *Proceedings of the National Fusarium Head Blight Forum, 2003*. East Lansing, MN, USA: Michigan State University, 129–32.
Del Ponte EM, Fernandes JMC, Bergstrom GC, 2007. Influence of growth stage on *Fusarium* head blight and deoxynivalenol production in wheat. *Journal of Phytopathology* **155**, 577–81.
Goswami RS, Kistler HC, 2004. Heading for disaster: *Fusarium graminearum* on cereal crops. *Molecular Plant Pathology* **5**, 515–25.
Gourdain E, Rosengarten P, 2011. Effects of infection time by *Fusarium graminearum* on ear blight, deoxynivalenol and zearalenon production in wheat. *Plant Breeding and Seed Science* **63**, 67–76.
Hallen-Adams HE, Wenner N, Kuldau GA, Trail F, 2011. Deoxynivalenol biosynthesis-related gene expression during wheat kernel colonization by *Fusarium graminearum*. *Phytopathology* **101**, 1091–6.
Hart LP, Pestka JJ, Liu MT, 1984. Effect of kernel development and wet periods on production of deoxynivalenol in wheat infected with *Gibberella zeae*. *Phytopathology* **74**, 1415–8.
Ioos R, Belhadj A, Menez M, Faure A, 2005. The effects of fungicides on *Fusarium* spp. and *Microdochium nivale* and their associated trichothecene mycotoxins in French naturally-infected cereal grains. *Crop Protection* **24**, 894–902.
Lacey J, Bateman GL, Mirocha CJ, 1999. Effects of infection time and moisture on development of spike blight and deoxynivalenol production by *Fusarium* spp. in wheat. *Annals of Applied Biology* **134**, 277–83.
Leonard KJ, Bushnell WR, 2003. *Fusarium Head Blight of Wheat and Barley*. St Paul, MN, USA: APS Press.
McMullen M, Jones R, Gallenberg D, 1997. Scab of wheat and barley: a re-emerging disease of devastating impact. *Plant Disease* **81**, 1340–8.
Nicolaisen M, Suproniene S, Nielsen LK, Lazzaro I, Spliid NH, Justesen AF, 2008. Real-time PCR for quantification of eleven individual *Fusarium* species in cereals. *Journal of Microbiological Methods* **76**, 234–40.
Nielsen LK, Jensen JD, Nielsen GC *et al.*, 2011. *Fusarium* head blight of cereals in Denmark: species complex and related mycotoxins. *Phytopathology* **101**, 960–9.
Parry DW, Jenkinson P, McLeod L, 1995. Fusarium ear blight (scab) in small grain cereals – a review. *Plant Pathology* **44**, 207–38.
Simpson DR, Thomsett MA, Nicholson P, 2004. Competitive interactions between *Microdochium nivale* var. *majus*, *M. nivale* var. *nivale* and *Fusarium culmorum in planta* and *in vitro*. *Environmental Microbiology* **6**, 79–87.
Siou D, 2013. *Epidemic Development of Fusarium Head Blight on Wheat and Consequences of Interactions Between Species Within the* Fusarium *Complex*. Paris, France: Paris XI University, PhD thesis.
Stenglein SA, 2009. *Fusarium poae*: a pathogen that needs more attention. *Journal of Plant Pathology* **91**, 25–36.
Strange RN, Majer JR, Smith H, 1974. The isolation and identification of choline and betaine as the two major components in anthers and wheat germ that stimulate *Fusarium graminearum in vitro*. *Physiological and Molecular Plant Pathology* **4**, 277–90.
Xu XM, Nicholson P, 2009. Community ecology of fungal pathogens causing wheat head blight. *Annual Review of Phytopathology* **47**, 83–103.
Xu XM, Parry DW, Nicholson P *et al.*, 2008. Within-field variability of *Fusarium* head blight pathogens and their associated mycotoxins. *European Journal of Plant Pathology* **120**, 21–34.
Zadoks JC, Chang TT, Konzak CF, 1974. A decimal code for the growth stages of cereals. *Weed Research* **14**, 415–21.

Supporting information

Additional Supporting Information may be found in the online version of this article.

Figure S1. Visual symptoms of FHB on wheat kernels. Examples of wheat kernels collected from different spikes inoculated with fg178 (*Fusarium graminearum*) in 2011 at different dates (F0 to F28), and corresponding mean TKW.

Table S1. Eluent conditions used in the UPLC-UV-MS/MS mycotoxin quantification.

Table S2. Multiple Reaction Monitoring (MRM) transitions and their corresponding optimized parameters.